NOTES AND CORRESPONDENCE

Inexpensive Time-Lapse Digital Cameras for Studying Transient Meteorological Phenomena: Dust Devils and Playa Flooding

RALPH D. LORENZ

Space Department, Applied Physics Laboratory, The Johns Hopkins University, Laurel, Maryland, and Lunar and Planetary Laboratory, The University of Arizona, Tucson, Arizona

BRIAN JACKSON

Lunar and Planetary Laboratory, The University of Arizona, Tucson, Arizona

JASON W. BARNES

Physics Department, University of Idaho, Moscow, Idaho

ABSTRACT

The authors describe the design and performance of inexpensive and compact time-lapse cameras suitable for field deployment in remote locations for long periods and their application to studying two time-variable meteorological phenomena in arid regions: desert dust devils and transient flooding of playa lakes. The camera units (with a total parts cost of ~$80) are based around commercial "point and shoot" digital cameras, storing ~1500 images on a solid-state memory card over a period between an hour to several months powered by alkaline batteries. A microcontroller can trigger image acquisition based on sensor inputs or at regular intervals. Some example results are presented, showing an association of cumulus clouds with thermals from dust devils, a region of dust enhancement around a dust devil, and a dramatic range of conditions at Racetrack Playa in Death Valley National Park. Alternative systems and applications are also discussed.

1. Introduction

Many phenomena of geophysical or meteorological interest are rare and short lived, making their observation require expensive effort and patience or luck. However, developments in consumer electronics—in particular, the availability of inexpensive digital cameras with large memory capacity—make it now affordable to deploy self-contained imaging systems in the field that can acquire large numbers of images over long periods.

Although this approach does not permit image analysis in real time but only after the system is retrieved and the data transferred to a computer, it provides scope for considerable savings in labor, in that the observation time can be a large multiple of the deployment time, and the inspection of image data can be performed efficiently in comfortable conditions (or even automatically). Further, the digital image record can permit quantitative analyses with more fidelity and fewer (or, at least, more quantifiable) biases than visual observation in real time by human observers.

In this paper, we describe a suite of designs of time-lapse camera units and their performance in the field. We consider two applications. First is the study of desert dust devils, dry convective vortices rendered visible by lofted dust (e.g., Balme and Greeley 2006). These features, a nuisance for outdoor activities and occasionally responsible for structural damage and aircraft accidents (Lorenz and Myers 2005), typically last only a few minutes. Hot and tedious visual surveys have determined their general diurnal and seasonal pattern of activity, but high-quality data on their sizes, morphologies, and recurrence intervals are lacking. Time-lapse camera surveys

Corresponding author address: Ralph D. Lorenz, Space Department, Applied Physics Laboratory, The Johns Hopkins University, 11100 Johns Hopkins Road, Laurel, MD 20723.
E-mail: ralph.lorenz@jhuapl.edu

offer the prospect of inexpensively producing strong statistics. A second application relates to the transient flooding of playa lakes. These features are dry for the vast majority of the time, but occasional precipitation can cause them to be water covered for hours to days. Understanding the occasionally striking geomorphology of these features requires that their hydrology be understood. For playas in remote locations, characterization of the playa state (e.g., dry, flooded, frozen, or muddy) is efficiently performed with time-lapse observations.

2. Camera technology

Imaging is a powerful means of obtaining data on many phenomena. In locations with modest infrastructure (AC power and shelter), video surveillance cameras have occasionally permitted interesting geophysical observations. Two examples are particularly interesting. First was the 1995 Kobe earthquake in Japan, wherein the motions of shopping carts relative to the floor was recorded by convenience store security cameras; in this instance, the carts were static and the ground motion was what was measured, allowing the fault location and its motion to be inferred (Kikuchi 1995). A second example was the detection of a meteor fireball by a parking lot surveillance camera in Nuuk, Greenland (Pedersen et al. 2001); in fact, security camera records have now been used several times to help reconstruct meteorite trajectories.

Video, however, is not convenient for remote observing stations and its frame rate is higher than ideal for many applications. PC-controlled webcams are a good model of the desired capability for many geophysical monitoring projects wherein intervals of minutes or hours can be appropriate but also require shelter and AC power (although, with an Internet connection, they have the powerful additional ability to be accessible remotely). A modified digital camera can provide webcam-like digital imagery, yet in a compact battery-powered package suitable for field installation. Modern digital cameras, writing to solid-state memory cards with capacities in the hundreds of megabytes or several gigabytes are now able to store hundreds or thousands of high-quality images, a far cry from the 36-shot reel of 35-mm film that was the state of the art for inexpensive cameras two decades ago.

The modifications to the camera are relatively straightforward, although they require customization or experimentation for the particular camera model (product turnover in consumer electronics being very rapid, a given model may be discontinued after only a year or two of sales). The principal modification is to trigger the shutter: an Internet search for "hacking cameras" will provide many detailed examples. Some cameras have

provision for a cable or infrared remote trigger, which can be exploited. More typically, the camera case must be opened and the shutter switch identified. The switch contacts can be bridged, typically by an opto-isolator or a transistor (or conceivably an electromechanical relay) such that an external 5-V logic pulse can trigger the shutter. For short intervals between frames (e.g., up to 1 min), a simple 555 timer chip is an inexpensive way of generating regular shutter pulses. Although simply "hotwiring" the shutter this way can allow short time-lapse sequences to be acquired immediately after the camera has been turned on, it is typical for cameras to power themselves down after a period of inactivity, with this "auto shut-off" feature typically being employed to save battery energy. Thus, it is usual for another switch to have to be activated to wake up the camera.

Because of the need to trigger two switches (and possibly a power relay; see later) and to have arbitrary long intervals between images, we use a small microcontroller to generate the pulses. A variety of devices could be used; we have found the PICAXE-08M (Revolution Education, United Kingdom) to be ideal; it can be programmed in a simple Beginners All-purpose Symbolic Instruction Code (BASIC) language, has four input–output lines (allowing, e.g., one for a sensor input, two for camera controls, and one for camera power), and costs under $4. Use of a microcontroller allows for substantial flexibility; for simple fixed-delay time-lapse work, the interval can be altered in software without making hardware modifications. Arbitrarily complex image sequences can be constructed (e.g., sets of three images 10 s apart, sets to be acquired at 10-min intervals). Finally, sensor-triggered image acquisition can be performed (e.g., to image only when it is windy or humid or when a pressure transient suggests the presence of a dust devil; e.g., Ringrose et al. 2003; Wagstaff 2009); in fact, variants of the arrangement described here are sold commercially as "trail cameras" for wildlife surveillance. Typically costing $200, these are often equipped with infrared motion triggers and flashes to capture images of wildlife at night. During the revision of this article, a comparable camera system (the Brinno GardenWatchCam, sold notionally for time-lapse observations of horticultural changes; available online at http://www.brinno.com) has become commercially available; because it lacks a motion trigger, it is more suitable for the meteorological applications here. Some more expensive time-lapse camera installations (see, e.g., online at http://www.harbortronics.com), based around digital single lens reflex (SLR) cameras, can provide much higher-quality imagery, albeit with larger housings and at rather higher cost. It should be borne in mind that the total cost of an investigation involving field deployment may exceed
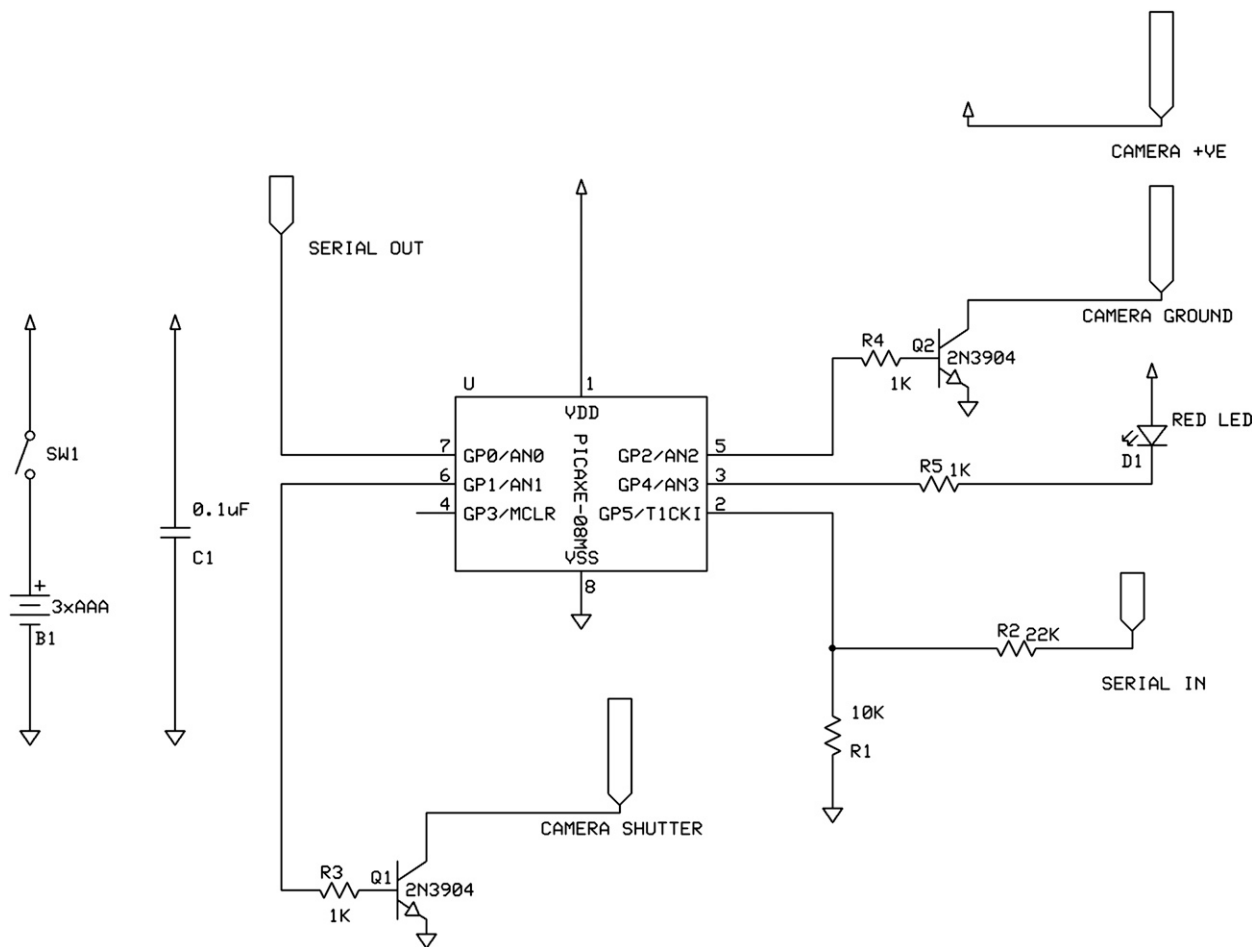
FIG. 1. Circuit for the Flycam trigger (the basic circuit for the VQ1005 is identical). The serial in and out connections are to permit programming of the PICAXE chip. The indicator light-emitting diode (LED) is optional: that pin on the microcontroller can instead be used for a sensor input to trigger camera operation.

the cost of the camera hardware, and thus compromising reliability to reduce hardware cost may be a false economy. However, in the present instance, the equipment budget was highly constrained, and the equipment had to be very small to avoid an adverse impact on the visual appearance of Racetrack Playa, a noted tourist site; thus, we experimented with small cameras rather than SLRs.

We conducted initial experiments with a Flycam-One (ACME GmbH, Germany), a small ~$90 camera presumably based around a cell phone camera platform and marketed for use in radio-controlled aircraft. This device records a 640 × 480 pixel color image to a Secure Digital (SD) memory card. The system has four buttons (of which, one wakes the camera up and another triggers the shutter) and uses an internal 3.7-V battery. The two switches were bypassed with 2N3904 transistors, which were triggered by PICAXE outputs (see Fig. 1). Although there was some initial success, prolonged camera operation using a 4.5-V supply (3 AA cells, which is

convenient for driving the PICAXE) caused permanent hardware failure of the memory cards. More elaborate power supply design could avoid problems. It was also found that partial image corruption sometimes occurred with many pixels set to yellow or cyan; although the cause could not be identified with confidence, it never occurred with manual operation of the shutter switch, so it may have been some kind of high-frequency noise from the PICAXE. Finally, it was noted that camera operation at voltages below about 3.4 V caused soft failure of the memory card (corruption of the file system leading to loss of data, but after reformatting the card could be reused). Again, careful power supply design might alleviate the problems. During these early experiments, some promising results of observing dust devils and at Racetrack Playa were obtained. However, new camera technology became available, with higher-resolution images at a lower camera cost, so experiments with the Flycam were discontinued.

New experiments have taken place with the Vista-quest VQ1005 camera. This product comes attached to a keychain and is slightly larger than a matchbox. The Vistaquest camera is remarkable in being little more expensive ($25) than the 512-MB SD memory card on which it can record its images. The camera takes good-quality pictures at resolutions of 1280×1024 pixels with a complementary metal oxide semiconductor (CMOS) imager with F/2.8 optics and is easy to dismantle and modify, but it has some peculiar features, doubtless to keep it both compact and cheap.

Like the Flycam, the VQ1005 stores its images (which can be at 640×480 or 1280×1024 or oversampled at 1600×1200) as JPEG files: typically about 2500 images can be stored on the memory card at the native 1280×1024 pixels. Also similar to the Flycam, the system does not record an image if the scene is too dark (the VQ1005 will perform autoexposure between 1/15 and 1/1500 s).

The camera is nominally powered by a single AAA cell. When switched on (accomplished by triggering the mode/power switch for 5 s) it draws a substantial 800 mA: even a fresh alkaline AAA cell with an open circuit voltage of >1.500 V may drop to 1.47 V. If the supply voltage drops below about 1.45 V, the camera powers off. This means that only about 10%–20% of the total battery energy can be used, compared with the energy to a more typical discharge voltage of 1.2 V. A more remarkable (negative) feature of the camera is that, even in standby mode, the camera draws about 2 mA.

However, it is reasonably straightforward to disconnect the 1.5-V battery from the camera using a relay triggered by the microcontroller, such that the standby energy consumption of the camera is reduced to zero. The typical sequence of operations commanded by the microcontroller (connected with 2N3904 transistors to the mode switch and shutter switch, with another transistor driving a relay) is (i) wait desired interval; (ii) energize relay to connect the 1.5-V battery to the camera; (iii) generate 5-s pulse on mode switch transistor to wake camera up; (iv) generate 1-s pulse on mode switch to set 1280×1024 pixel mode, or different pulse sequences could be used here to set lower or higher resolution; (v) generate 0.5-s pulse on shutter switch to acquire image; (vi) wait 5 s for safe file writing; and (vii) generate 5-s pulse on mode switch to put camera back to sleep. Because the entire sequence takes about 10 s, about 2 mA h^{-1} of energy from the 1.5-V supply is used. Experiments have shown that a fresh alkaline D cell, with a nominal capacity of ~20 000 mA h^{-1}, can support about 2500 shuttering sequences, as long as there is more than a minute between them (it will be recalled that battery capacity depends on discharge rate). This is approximately the number of images that can be stored

on a single memory card, although under typical mid-latitude conditions only about 1600 images of this number will be recorded, the other ~900 being too dark. If the relay is omitted, such that the camera is always on standby power, only a couple of weeks of operation are possible on a D cell (regardless how many images are actually acquired).

For field deployment, the camera is removed from its casing to solder connections to the circuit board for the battery, shutter, and mode switch, and mounted with adhesive behind a transparent plastic window in a black Acrylonitrile-Butadiene-Styrene (ABS) plastic case. This case also holds the camera battery, the microcontroller/transistor circuit board (an inexpensive "proto board" is available that is large enough to accommodate the programming connector for the PICAXE and the transistors for camera interfacing), and a separate 3-AA or 3-AAA cell power supply for the PICAXE (see Fig. 2). The PICAXE uses only a few mA when operating, but in sleep mode (which we use for the interval between images) it draws less than 100 μA, so it can operate for many months on the ~1000 mA h^{-1} available from AA cells. To minimize visual impact in the field, the case was sprayed with textured earth-toned paint. No specific measures were adopted to exclude moisture; in the arid regions associated with the present applications no moisture problems were encountered.

As described in the subsequent two sections, the cameras appear to have functioned adequately at least a few degrees below freezing and at temperatures of 40°C or more. The major difficulty encountered, in trials not reported in the following sections, has been unexpected data corruption associated with battery undervoltage. This has been successfully mitigated by several approaches. The microcontroller can compare its supply voltage with a reference and veto image acquisition if the voltage drops unacceptably. A regulated supply is an alternative (the Vistaquest camera normally uses a single AAA cell, so regulating the 4.5-V microcontroller supply to 1.5 V using an adjustable regulator such as LM317 is an effective, if slightly energy inefficient, approach); newer step-up regulators such as the LTC3429 may also be a useful solution. Finally, a simple strategy to use a fresh set of batteries each mission and limit the camera to acquire a fixed number of images (known empirically not to cause the voltage to drop) and then stop. There is of course a trade-off between extracting the maximum number of images possible with a given energy source and the effort one is prepared to devote to the challenge; this trade-off determines which of these approaches is adopted. We may note here also that, because the camera and a small battery can be assembled with a mass of only a few tens

FIG. 2. Layout of VQ1005 camera unit. At left is alkaline D cell to power camera. Next is camera itself [case removed, so circuit boards are exposed, showing liquid crystal display (LCD) status display]. A wire to the mode switch terminal from the microcontroller board is arrowed. At lower right is the microcontroller board with switching transistors, and above that is the 3-AAA cell power for the microcontroller.

of grams, it can be lofted by a small balloon (where it has been used for study of dry playa surfaces; C. McKay 2009, personal communication) or by a kite; a Web search on ''kite camera'' will yield many successful experiments. Similarly, a package need not be left unattended in the field but can be unobtrusively mounted on a vehicle to document field excursions or similar activities.

3. Application to dust devil surveys

Dust devils are desert whirlwinds rendered visible by lofted dust. Although field surveys (e.g., Sinclair 1969; Fitzjarrald 1973; Snow and McCLelland 1990; Oke et al. 2007) agree on the diurnal pattern of activity, the absolute numbers of dust devils in surveys vary widely, possibly as a result of different detection thresholds among the observers and the strong increase in number of smaller dust devils. In that connection, although a truncated exponential size distribution has been advocated on the basis of the crudely binned size statistics obtained by visual observers (Kurgansky 2006), higher-quality data are needed to discriminate such an exponential description from, for example, a power law.

Dust devils can occur in a variety of morphologies (e.g., Balme and Greeley 2006): wide cones to tall and slender columns to irregular. Columns may tilt appre-

ciably because of wind shear, and the dust devil as a whole may move at a speed different from the ambient wind. Correlation of these morphologies with meteorological conditions has so far been only anecdotal and is complicated by the fact that an individual dust devil may evolve in shape and speed, which may confound a field observer's efforts to classify the dust devil quantitatively. A time-lapse camera survey would allow robust statistics on these aspects of dust devils to be compiled and related to ambient meteorological conditions.

Finally, it has been suggested (e.g., Ryan and Carroll 1970) that there may be a short-term periodicity in dust devil occurrence (on the order of 10–20 min), perhaps because of activity draining the near-surface boundary layer of the hot air that powers the devils or perhaps because of some feedback involving lofted dust. However, visual surveys to date have generally only recorded statistics of dust devils in 1-h time bins, making detection of such periodicity impossible.

As a trial, we set up a single Flycam-based camera near Gates Pass in Tucson, Arizona, looking westward toward the Avra Valley area surveyed by Sinclair (1969). This camera was set to record a 640×480 pixel image every minute. Although the valley was some 10 km away, several large dust devils were detected. Meteorological conditions were sufficiently humid that,
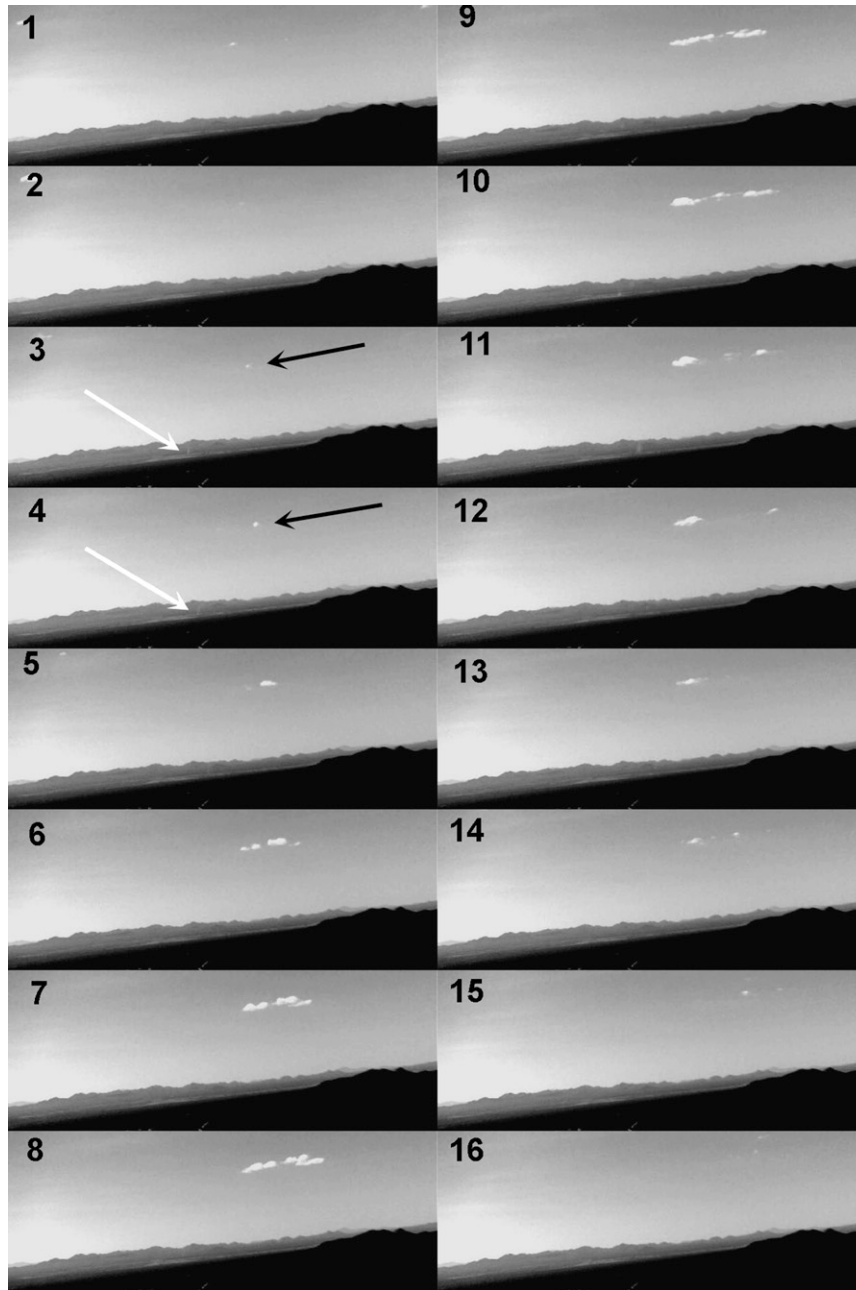
FIG. 3. A sequence of 16 images spaced by ~1 min at Gates Pass, near Tucson, AZ, looking west to Avra Valley. Sequence begins at ~1430 h on 18 Sep 2007. Note the formation of small cumulus clouds (black arrow), apparently by thermals associated with a dust devil (white arrow).

although a hot and overall dry day, lofted air was able to condense and intriguingly small cumulus clouds formed contemporaneously and almost directly above several dust devils (see Fig. 3).

A second trial was performed in May 2008, with a Vistaquest camera set to acquire images at 45-s intervals. This camera was set up near the Arizona Desert Museum and thus is rather closer to the Avra Valley plain where the dust devils form. An example set of images is shown in Fig. 4 and nicely shows the progression of a dust devil across the scene at a more or less constant velocity. The fixed location means that few features in the image change from one frame to the next and illumination changes only slightly. Thus, successive
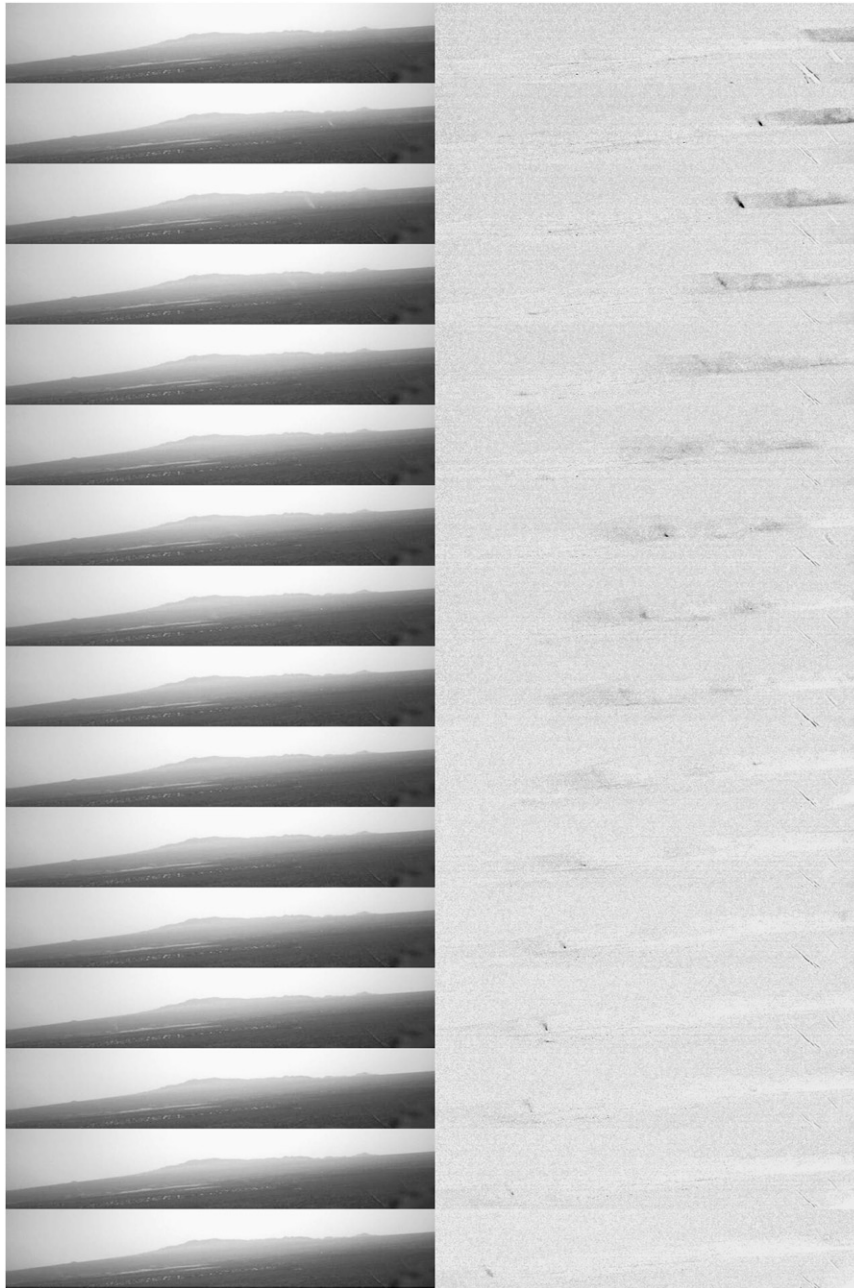
FIG. 4. A sequence of cropped images, 45 s apart, acquired in Avra Valley (looking south-west) starting at 1305 LT on 20 May 2008. At right is the same sequence but showing only the difference between each image and the average of the set, thereby enhancing the changing feature—specifically the dust devil, which is visible in the difference image for nearly the entire set, whereas it is only prominent in the originals in a few frames. Notice the consistent motion across the scene and the variable strength of the devil itself (which would be difficult to characterize quantitatively by eye). Note also the broad perturbation around the devil: pre-sumably, lofted dust. The persistent diagonal line at right is a blade of grass in the foreground, which is moved by the wind and thus appears in difference images.

images can be differenced in postprocessing, or the average frame from a batch of images subtracted from each, to leave the changing portion of the image: in this case, the dust devil. This approach has been used on sequences of images to detect dust devils observed on the surface of Mars by the rover *Spirit* (Greeley et al. 2006). It is seen in Fig. 4 that, in addition to the dust devil itself, there is a broader region of dustiness, perhaps either disturbed by the radial flow into the dust devil or even dust lofted by the devil and ejected at its top.

Although not shown in Fig. 4 (where the images have been cropped to the region of interest containing the dust devil), the differenced images showed evidence of motion in the sky, even though no clouds were apparent in the raw images, or to a human observer on site at the time. The contrast enhancement provided by differencing evidently made visible small amounts of cloud or dust opacity that could act as wind tracers in the sky.

Clearly, then, the instrument described here can be used for systematic surveys and in principle can have a lower opacity threshold than a fatigued human observer might. A variety of field observing strategies are possible. In a typical deployment, one might spend an hour deploying several (e.g., ~4) cameras at the beginning of the day, an hour retrieving them at the end of the day, and then an hour to download and study the images. Even a manual inspection of such an image sequence is an efficient approach in that one can browse through an image sequence at one frame every second or so. Additionally, there are now machine vision algorithms developed for real-time dust devil detection on the Mars exploration rovers (Castano et al. 2008) that can automatically process images and identify those that contain dust devils. Thus, for ~3 h of effort, one obtains ~36 station hours of observation, an effective force multiplier.

Another approach might be to set up cameras to record for 5 days, with a cadence of 1–2 min. This provides an even higher force multiplier for the effort, at the expense of poorer time resolution (resulting in ambiguity of discriminating long-lived but moving devils from separate but short-lived devils). Even if the interval between images is longer than the typical lifetime of an individual dust devil and thus is an incomplete census, a regularly spaced image sequence still provides an unbiased means of evaluating the variation with time of dust devil numbers, size, dust loading, and morphology and the correlation between these variables. Remarkably, data on the diameter distribution of dust devil diameters are better for Mars (Lorenz 2009), where rover camera data have been systematically inspected with image analysis tools has, than on Earth, where the only published surveys are those done visually in the field. The combination of such data with meteoro-

logical context measurements—and desirably with in situ measurements of the dust devils themselves—would be particularly useful.

4. Playa lake observations

Observing dust devils was the principal motivation behind developing these cameras. However, dust devil activity is minimal during winter, and thus a second application was found to field-test the camera during the winter months. This relates to the transient flooding of Racetrack Playa in Death Valley National Park. This is a 4.5 km × 2 km lake bed at an elevation of 1130 m and may be wetted only for a few days during a typical year, because the park as a whole is very dry (Roof and Callagan 2003). In this respect (and several others), it may resemble some lakes on Saturn's moon Titan (Lorenz et al. 2009), where evaporation also exceeds precipitation by orders of magnitude, although on that cold, distant world the fluid being rained and evaporated is methane (e.g., Lorenz and Mitton 2008). It is exceptionally flat (the south end is only a few centimeters lower in elevation than the north) and is of mixed sand–silt–clay composition, usually with striking but small desiccation polygons. It is distinguished (e.g., Sharp and Carey 1976) by the presence of some dozens of rocks (usually cobbles or small boulders), which are very distinct against the very uniform playa (Fig. 5) and often appear at the end of trails or furrows in the playa surface. These trails suggest that the rocks have moved across the surface at some speed when the playa was wet. Much attention has been directed toward documenting the rocks and their movements (e.g., Kirk 1952; Sharp and Carey 1976; Reid et al. 1995; Messina and Stoffer 2000), which are apparently caused by wind and possibly facilitated in some instances by ice formations around the rocks. However, in situ meteorological data at the playa (reached by a sometimes-closed 25-mile dirt road) are not available and observations of how frequently the playa is flooded, muddy, or frozen are lacking.

Because Racetrack Playa is a site of outstanding natural beauty and formally a Wilderness Area, equipment must therefore be unobtrusive and set up off the playa itself. After approving the location of our camera with National Parks Service staff and acquiring the necessary permit, we performed an initial trial with a C-cell-powered Flycam system. This was packaged in a black die-cast aluminum box 6 cm × 12 cm × 20 cm and set on the ground in the cliffs at the south end of the playa (visual-impact considerations precluded the use of a tripod). Over the observation period from 29 November 2007 to 3 March 2008, some 1100 images were acquired with a nominal spacing of 1 h. Some images were partially

FIG. 5. The normal condition of Racetrack Playa: image 384, acquired in late January 2009, looking north from the cliffs above the south edge of the playa. The rock formation ''The Grandstand'' is visible two-thirds of the way from left to right, just above the horizontal edge of the playa, halfway up the image. Five rocks on the playa are visible in the foreground.

corrupted by a file system problem with low-voltage operation of the SD memory card to which the images were recorded, but the state of the playa could nonetheless be evaluated and three episodes of wetting were noted.

A subsequent observation was performed with a Vistaquest camera between 3 December 2008 and 3 March 2009, with an interim change out of the camera allowing a higher frame rate of $\sim$2 h^{-1}. Image quality was much better than for the Flycam, with no significant image corruption, as well as higher intrinsic resolution. About a half-dozen images were truncated, perhaps because of issues with low-temperature operation. The color balance was also suspect on one image (the overall appearance was pink); this is likely due to poor performance of the automatic color balance in the camera in marginal dawn lighting conditions when the scene was white with snow.

For most of the observing period, the playa had its usual dry condition, with one brief dusting of snow circa 19 January. However, a more significant snowstorm passed through at the beginning of February 2009 (Fig. 6), and indeed some falling snowflakes appear, slightly blurred, in some images. One difficulty arises in variable weather conditions in that the images from this particular camera are not time stamped: one must infer an approximate date and time from the image file name (corresponding to

the ordinal number of the file being written to the memory card). In other words, image 0145 occurs between 0144 and 0146, and probably occurs 30 min (or whatever delay is implemented in the microcontroller) after 0144. However, if darkness caused by time of day or by heavy cloud brought the camera below the threshold at which it stores an image, there will be an undetermined number of image intervals between successive recorded image files (in a sequence of geological layers, the analogous discontinuity would be called an unconformity.) Thus, dates cannot always be determined with absolute precision, although we know from humidity and temperature measurements acquired with nearby dataloggers that were equipped with timestamps that conditions became suddenly humid and buffered around the freezing point, suggesting the presence of snow, on 6 February 2009.

Subsequent images (Fig. 6) show that the snow melts and the resultant shallow lake on the playa can be blown significantly by the wind (so-called wind set up) and the surface of the lake can be roughened significantly providing second indication in the image record of wind stress.

The following morning, the lake could be seen to be frozen. The lake texture was slightly different in the images from how it appeared when wind ruffled, but more robustly the features on the lake surface remained
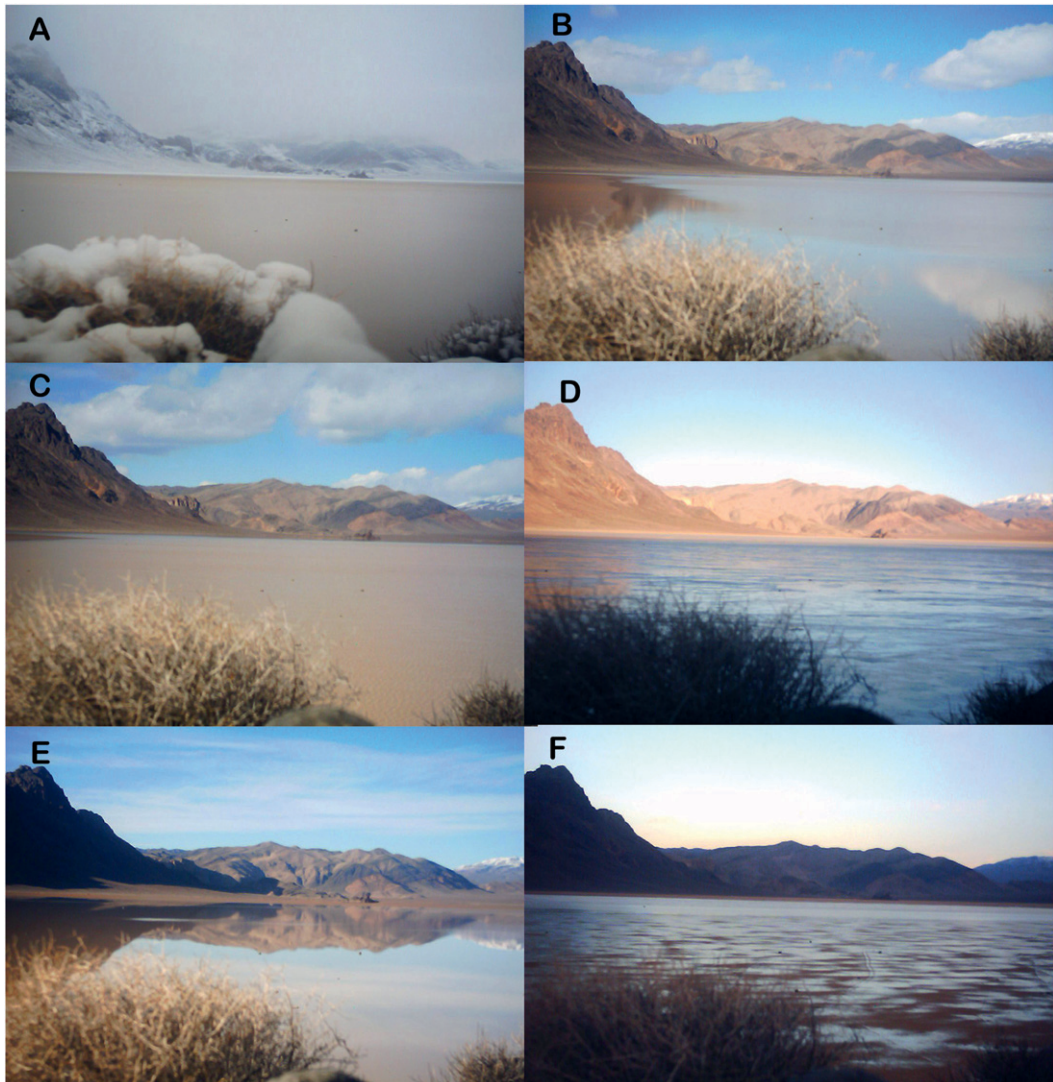
FIG. 6. (a) Image 445: the playa after a snowstorm. Note that the snow cover on the playa itself is rather thin, because the color of the playa mud can be discerned. (b) Image 476: the snow has melted and the playa is partly covered with water. The playa is exposed at left, and a narrow band of smooth water is evidenced at the edge by a mirror-like reflection of the distant skyline. To the right, the water surface is disturbed by wind. (c) Image 477: about 30 min after image 476. The playa is completely flooded, although the surface is disturbed by wind (individual ripples can be discerned at lower right). It seems likely that wind stress on the surface of the shallow lake (it is not so deep as to submerge the ~20-cm rocks in the foreground) pushes the water around, exposing the bed at the upwind side. (d) Image 490: early in the day following image 476. The surface of the playa lake is frozen (the surface patterns are identical in several subsequent frames, confirming that the textures are fixed and therefore due to ice, rather than wind effects). (e) Image 504: late in the same day. Conditions are evidently calm, as evidenced by the near-perfect specular reflection on the lake surface. (f) Image 553: a few days after image 504. Evaporation has nearly dried the lake out and the residual moisture forms semiregular patterns on the playa surface. The water or frost highlights some subtle playa textures, notably the parallel lines about 2/3 across the image delineating a rock trail.

identical in several frames spanning a couple of hours before they progressively disappeared through melting. Determining the lake to be frozen places a constraint on its energy budget as well as being of potential interest in the motion of the rocks on the playa in that ice sails may facilitate wind dragging on the rocks. Later that day, the ice had melted and wind stress on the lake was evidently minimal: the lake surface became a perfect mirror.

Finally, the progressive evaporation of the lake could be seen allowing constraints to be placed on the overall evaporation rate; in essence, the lake acts as a large, natural evaporation pan. Intriguing semiregular patterns

formed in the playa bed as drying of the playa became complete. Whether these patterns are purely ephemeral and stochastic or reflect some underlying (but invisible) variation in the character of the playa sediments cannot be determined, although repetition of the patterns on a subsequent wetting–drying cycle would support such a substrate control of the pattern.

Of course, it would be interesting to observe the rocks themselves in actual motion (and we note that the cameras used here are able to record short video sequences as well as stills; in the case of the Vistaquest camera, it would require only an additional couple of mode switch pulses in the microcontroller program). However, given that the rock movement episodes are only ~10 s in duration and surveys have indicated (e.g., Sharp and Carey 1976) that movements may take place perhaps one year in three, movement occurs only about one-millionth of the time. Thus, observations while rocks are in motion would likely require some kind of wind-triggered imagery: there is a fair probability that movement might in any case occur unobservably at night and that the conditions that cause movement (wet and wind) may tend to cause obscuration of the playa by spray or fog. However, regular imagery can at least permit the time of a movement event to be documented to a day or better, thereby allowing the conditions pertaining when the event occurred to be documented. Further, as we have shown here, imaging also permits the frequency and duration of various conditions (wet, frozen, etc.) of the playa to be quantified.

5. Conclusions

The memory capacity, low cost, and small size of digital cameras now permits large amounts of image data to be acquired in settings that were not previously feasible. Time-lapse imagery from such small cameras as those discussed here need not be acquired from fixed sites but can be taken through the windows of road vehicles or aircraft, or even from kites or balloons. From fixed sites, as described here, these inexpensive devices can open new windows into the study of time-variable meteorological phenomena.

REFERENCES

Balme, M., and R. Greeley, 2006: Dust devils on Earth and Mars. *Rev. Geophys.,* **44,** RG3003, doi:10.1029/2005RG000188.

Castano, A., and Coauthors, 2008: Automatic detection of dust devils and clouds on Mars. *Mach. Vision Appl.,* **19,** 467–482.

Fitzjarrald, D. E., 1973: A field investigation of dust devils. *J. Appl. Meteor.,* **12,** 808–813.

Greeley, R., and Coauthors, 2006: Active dust devils in Gusev crater, Mars: Observations from the Mars Exploration Rover Spirit. *J. Geophys. Res.,* **111,** E12S09, doi:10.1029/2006JE002743.

Kikuchi, M., 1995: A shopping trolley seismograph. *Nature,* **377,** 19.

Kirk, L. G., 1952: Trails and rocks observed on a playa in Death Valley National Monument, California. *J. Sediment. Petrol.,* **22,** 173–181.

Kurgansky, M. V., 2006: Steady-state properties and statistical distribution of atmospheric dust devils. *Geophys. Res. Lett.,* **33,** L19S06, doi:10.1029/2006GL026142.

Lorenz, R. D., 2009: Power law of dust devil diameters on Mars and Earth. *Icarus,* **203,** 683–684.

——, and M. J. Myers, 2005: Dust devil hazard to aviation: A review of United States air accident reports. *J. Meteor.,* **30,** 178–184.

——, and J. Mitton, 2008: *Titan Unveiled.* Princeton University Press, 243 pp.

——, B. Jackson, and A. Hayes, 2009: Racetrack and Bonnie Claire: Southwestern US playa lakes as analogs for Ontario Lacus, Titan. *Planet. Space Sci.,* doi:10.1016/j.pss.2009.05.012, in press.

Messina, P., and P. Stoffer, 2000: Terrain analysis of the Racetrack Basin and the sliding rocks of Death Valley. *Geomorphology,* **35,** 253–265.

Oke, A. M. C., N. J. Tapper, and D. Dunkerley, 2007: Willy-willies in the Australian landscape: The role of key meteorological variables and surface conditions in defining frequency and spatial characteristics. *J. Arid Environ.,* **71,** 201–215.

Pedersen, H., R. E. Spalding, E. Tagliaferri, Z. Ceplecha, T. Risbo, and H. Haack, 2001: Greenland superbolide event of 1997 December 9. *Meteorit. Planet. Sci.,* **36,** 549–558.

Reid, J. B., E. P. Bucklin, L. Copenagle, J. Kidder, S. M. Pack, P. J. Polissar, and M. L. Williams, 1995: Sliding rocks at the Racetrack, Death Valley: What makes them move? *Geology,* **23,** 819–822.

Ringrose, T. J., M. C. Towner, and J. C. Zarnecki, 2003: Convective vortices on Mars: A reanalysis of Viking Lander 2 meteorological data, sols 1–60. *Icarus,* **163,** 78–87.

Roof, S., and C. Callagan, 2003: The climate of Death Valley, California. *Bull. Amer. Meteor. Soc.,* **84,** 1725–1739.

Ryan, J. A., and J. J. Carroll, 1970: Dust devil wind velocities: Mature state. *J. Geophys. Res.,* **75,** 531–541.

Sharp, R. P., and D. L. Carey, 1976: Sliding stones, Racetrack Playa, California. *Geol. Soc. Amer. Bull.,* **87,** 1704–1717.

Sinclair, P. C., 1969: General characteristics of dust devils. *J. Appl. Meteor.,* **8,** 32–45.

Snow, J. T., and T. McClelland, 1990: Dust devils at White Sands Missile Range, New Mexico 1. Temporal and spatial distributions. *J. Geophys. Res.,* **95,** 13 707–13 721.

Wagstaff, K., 2009: Real-time detection of dust devils from pressure readings. NASA Tech Brief NPO-44724, NASA Tech. Briefs, 6.